Curvature Vector Flow to Assure Convergent Deformable Models for Shape Modelling

Debora Gil and Petia Radeva

Computer Vision Center (CVC), Edifici O, Campus UAB
08193 Bellaterra, Barcelona, Spain.
{debora, petia}@cvc.uab.es
fax/tel: 93 581 16 70 /93 581 30 36 *

Abstract. Poor convergence to concave shapes is a main limitation of snakes as a standard segmentation and shape modelling technique. The gradient of the external energy of the snake represents a force that pushes the snake into concave regions, as its internal energy increases when new inflexion points are created. In spite of the improvement of the external energy by the gradient vector flow technique, highly non convex shapes can not be obtained, yet. In the present paper, we develop a new external energy based on the geometry of the curve to be modelled. By tracking back the deformation of a curve that evolves by minimum curvature flow, we construct a distance map that encapsulates the natural way of adapting to non convex shapes. The gradient of this map, which we call curvature vector flow (CVF), is capable of attracting a snake towards any contour, whatever its geometry. Our experiments show that, any initial snake condition converges to the curve to be modelled in optimal time.

1 Introduction

Shape modelling arises in many fields of computer vision and graphics [13], [8], [25], to mention just a few. The most efficient way of producing smooth models of shapes is by means of a snake [14], [1], [2]. Snakes are curves that minimize an energy functional. In classic snakes [14], this functional splits into an external energy, depending on the set of points to be approached, and an internal one that serves to smoothly interpolate the curve to be modelled when no information is available. Geodesic snakes [1], [2] blend both the internal and external energies and seek for the curve of minimal length in a Riemmanian manifold with the external energy as metric. In any case the minimum of the energy functional is obtained by gradient descent of an initial contour. Hence the definition of the external energy is crucial for a successful model of the shape.

Distance maps are one of the most used external energies, simple and quick to compute. Curves of level zero correspond to the contour of interest and the snake moves in the direction opposite to the gradient of the distance map. Unfortunately, the geometry of the curve of level zero may produce maps with null

* This work is partially supported by the "Ministerio de Ciencia y Tecnologia" grant TIC2000-1635-C04-04.

gradients along some curves. The snake gets caught in these local minima and produces a wrong model of the shape. There are several ways of addressing this problem. We can initialize the snake close to the final shape so that we make sure that it is far away from these local minima. This is certainly not a very elegant approach for automated procedures. Some authors [3], [20] suggest searching for the global minimum of the energy, but global minimums of real images are hard to find in an efficient way without manual intervention. The most sensible solution up to now consists in using the Gradient Vector Flow (GVF) or the Generalized Gradient Vector Flow (GGVF) to obtain a regularized version of the gradient of the external energy [22], [24], [23] that only admits isolated zeros. The technique succeeds in producing smooth gradients in the whole image that guide the snake to the final contour for a large variety of geometries. However the vector field obtained with GVF may have saddle points which also trap the snake. No technique will remove saddle points because they are inherent to the distance map. We need a new definition of the distance map.

The novelty of this work is that we study distance maps from a geometric point of view, which clearly shows the limitations of the current external forces. By means of the formulas developed, we build a new distance map to closed contours.

An analysis of the Euclidean distance map points out that propagating a shape with constant speed produces shocks in the map that difficult using its gradient as external force in the snake equation. In this paper we propose a distance map that takes into account the local geometry of the closed contour we want to approach. A back-tracking of the evolution of the contour of level zero by minimum curvature flow [17] is the natural geometric way of converging to non-convex regions. Since the PDE associated to this evolution is of elliptic type, we can assure that propagation of non convex regions will not develop shocks during the process. In this manner we build a distance map having the contour of level zero as unique local minimum. The gradient of the map, called Curvature Vector Flow, is capable of attracting any initial interior or exterior curve towards the contour of interest, independently of its geometric features.

Experiments done on synthetic shapes and contours extracted from real images, show that CVF adapts snakes to any geometry of the curve to be modelled, provided the initial snake lies completely either in the interior or exterior of the shape to model. Comparing to other external forces (GVF and Euclidean distance map), not only is CVF the most efficient and accurate but also the graphs of the snake total energy present a smoother asymptotic behavior. This minimizes the snake oscillation in a neighborhood of the equilibrium state and provides CVF with a stop criterion either in terms of the magnitude of the energy or in terms of stabilization of the iterative numerical scheme. Shapes that CVF yields represent accurate smooth models of the contours. Further, using B-spline parametric snakes a compact representation is obtained.

The paper is organized as follows: the theoretical analysis of shape propagation is given in Section 2; advantages and drawbacks of the Euclidean distance map and GVF are described in Sections 2.1 and 2.2, respectively; the formu-

lation of CVF in Section 2.3. Applications to shape modelling are presented in Section 3 and, finally, Section 4 is devoted to conclusions and further research.

2 Shape Propagation

Distance maps encode the evolution of the curve of level zero, γ_0, under a geometric flow defined, generically, by a parabolic PDE:

$$\gamma_t(u,t) = \beta(u,t)\overrightarrow{n} \ . \tag{1}$$

with initial condition $\gamma(u,0) = \gamma_0(u)$ a closed curve and $\overrightarrow{n}$ denoting the unit inward normal. Each level curve of a given distance, d, corresponds to the solution to (1) at time $t = d$. This point of view, reduces the study of distance maps to the analysis of the propagation of the zero level curve governed by means of a geometric flow. We will use the machinery developed in [4] in order to study the drawbacks of the Euclidean distance map and define a more natural way of propagating shapes that will produce distance maps capable of guiding a snake to any closed curve. Since a plane curve is defined, up to rigid transformations, by its unit tangent, a pleasant way of handling geometric flows is by means of the equation of the angle of the unit tangent, θ, in the arc length, s, parameterization. The advantage of this formulation is that we reduce the study of the properties of (1) to the analysis of a single equation, so that standard results on PDE's can be applied. The parabolic PDE for θ when the curve solves (1) is given by:

$$\theta_t(s,t) = \partial_s(\beta) + \left(\int_0^s \beta\theta_s ds\right)\theta_s \ . \tag{2}$$

with initial condition the angle of the unit tangent, θ_0, of the initial curve. An important remark is that the first order term arises due to the change of parameter, and, hence, it is present in any geometric flow.

2.1 Euclidean Distance Maps

In Euclidean distance maps, propagation of the initial curve, γ_0, is equivalent to mathematical morphology with a circle of radius 1 as structural element. Erosion corresponds to the inward propagation and dilation to the outward one. Hence the geometric flow associated [12] [18] is given by:

$$\gamma_t = \pm\overrightarrow{n} \ .$$

The minus sign corresponds to the dilation and the plus to the erosion. Since, in this case, $\beta = \pm 1$ is constant, the corresponding equation (2) for θ is simply:

$$\theta_t(s,t) = \pm(\int_0^s \theta_s ds)\theta_s \ . \tag{3}$$

This equation is a first order non-linear PDE that is solved [7] by means of the computation of the characteristic curves, that is, those curves in the s-t plane,

$\alpha(u)$, such that the function solving (3) keeps constant, that is $\theta(\alpha(u)) \equiv const.$ Assuming this last condition for $\alpha(u) = (s(u), t(u))$, we obtain that:

$$0 = \frac{d}{du}(\theta(s(u), t(u)) = t_u\theta_t + s_u\theta_s = t_u(\pm(\int_0^s \theta_s ds)\theta_s) + s_u\theta_s = (\pm t_u\theta + s_u)\theta_s \ .$$

Since the equality holds for all points in the characteristic, we have that α solves the first order PDE:

$$\pm t_u\theta + s_u = 0$$

And, consequently, its tangent vector fulfils the following system of ODE's:

$$\left.\begin{array}{l} t_u = \ 1 \\ s_u = \pm\theta \end{array}\right\}$$

Therefore, the characteristics through a point $(s_0, 0)$ are parameterized as:

$$\alpha(u) = (\pm\theta_0 u + s_0, u) \ .$$

where θ_0 equals $\theta_0(s_0, 0)$ and is constant along the characteristics.

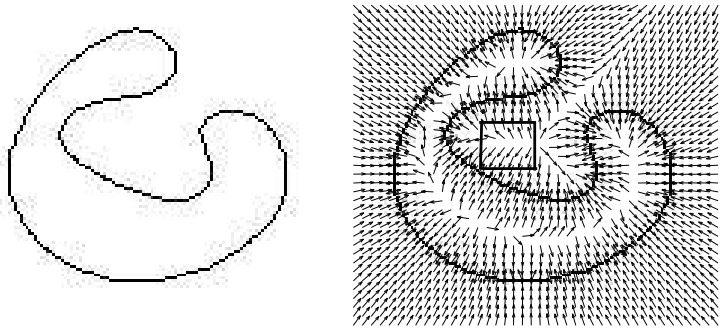

(a) (b)

Fig. 1. Highly non-convex curve (a) and gradient of Euclidean distance map (b).

This means that we have straight lines in a plane which slopes, $\theta_0(s_0)$, do not need to be a monotonous function of the curve parameter. Variation of the characteristics slope along the initial curve is given by the derivative of the angle θ_0'. Since the initial curve is parameterized by its arc length, we have that the sign of the curvature of the initial curve determines whether the slopes increase or decrease. For convex curves, characteristics slope are either increasing (inward propagation) or decreasing (outward propagation) along the curve. Hence, two different characteristics never cross during the curve propagation and the distance map is a smooth map. However, for non-convex shapes, changes in the

monotonicity of the slopes induced by the curve inflexion points make characteristics meet each other in finite positive time (squared region of fig. 1(b)) . At this time, the evolution of the angle develops a discontinuity or shock and the corresponding curve is not smooth any more. Indeed shocks in the angle domain translate into points or, even, curves where the gradient of the distance map cancels, that is, they correspond to crests and valleys of the distance map. Although this property is used in computer vision for extraction of shape skeletons [19], [21], it constitutes a main hindrance for shape modelling with snakes. Highly non-convex shapes (see fig. 1(a)) with the angle turning around more than π between two consecutive inflexion points produce distance maps with crests of positive slope (fig. 3(a)). These crests and valleys induce local minima in the snake energy functional that our deformable model, which seeks for zeros of the energy gradient, will never cross.

The best approach up to our knowledge to overcome the null gradient problem along curves is by means of the use of a regularized gradient (that only cancels at isolated points) as external force. Such regularization is obtained by means of the GVF [22] or its generalized faster version GGVF [24].

2.2 Gradient Vector Flow and Saddle Points

The GVF/GGVF technique [22], [24] consists in substituting the gradient of the external energy, ∇E_e, by the vector field $v(x)$ that is the steady-state of the reaction-diffusion vector equation:

$$u_t = g(|\nabla E_e|)\nabla u - h(|\nabla E_e|)(u - \nabla E_e) \quad \text{with } u(x,0) = \nabla E_e \tag{4}$$

The weighting functions, $g(\cdot)$ and $h(\cdot)$ are monotonically non-increasing and non-decreasing functions of the norm $|\nabla E_e|$, respectively. An important remark is that $h(0) = 0$. In this manner, the equilibrium vector field smoothly extends ∇E_e, thanks to the Laplacian, keeping close to the original gradient when it is significant enough. It can be used either to extend the edge map to the whole image or to regularize a gradient of a distance map. The main difference between GVF and GGVF is that the latter field keeps enough force as to drive the snake until the edge.

Notice that, in any of the two cases (GVF or GGVF), at parts of null gradient the equilibrium point is an harmonic function. Harmonic functions [16] do not admit accumulation of zeros and, thus, our vector field v will only have isolated points with $|v| = 0$. This important feature solves the problem of the distance map null gradient along curves (fig. 2 (b)). However, in both cases the geometry of the contours introduces saddle points in the vector field v, as the close up in fig. 2 (c) illustrates. These false minima of the snake energy trap, once again, the snake and prevent the deformable contour from entering into concave regions where the angle of the unit tangent, θ, turns around more than π.

For regularization of gradients of Euclidean distance maps, saddle points appear because of shock formation during the propagation of the curve of level zero. In the case of extension of image gradients we find a similar problem. The

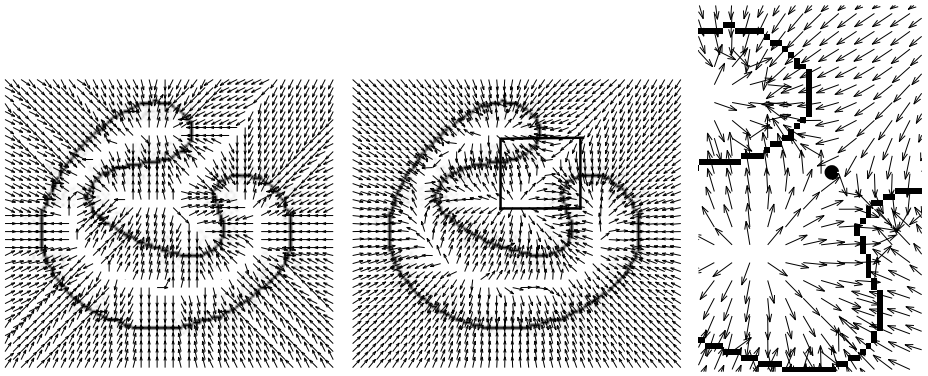

(a) (b) (c)

Fig. 2. Gradient of Euclidean distance map to non-convex curve (a), GGVF (b) and saddle point of GGVF (c).

Laplacian is an isotropic linear constant way of extending information. Therefore in every image region such that the contour/edge of interest is concave and the angle of the image gradient (parallel to the unit normal of the curve) turns more than π, two opposite directions meet (fig. 2 (c)) and we have a saddle point.

In order to eliminate saddle points we need changing the propagation of shapes, so that the geometry of the contour to be extended is taken into account.

2.3 Curvature Vector Flow

Let us analyze the problem of the Euclidean distance map. From an analytic point of view, we see that equation (3) is a non-linear first order PDE, prone to develop shocks during the evolution. From a geometric one, it lies on the fact that we are propagating the curve at constant speed whatever its geometric features. In other words, the structural element used in the mathematical morphology is a circle of constant radius, which means that all points in the curve travel equal distance at the same time. We argue that the evolution should consider different metrics depending on the local geometry around each point so that structural circular elements of non constant radius are used. And what characterizes the local geometry of a curve better than curvature?. We propose [5] a distance map based on the Mean Curvature Flow, that is, the evolution of the curve of level zero under the PDE given by:

$$\gamma_t = \kappa \overrightarrow{n} \ . \tag{5}$$

This equation makes points on the curve travel a distance that depends on the magnitude of the curvature, the higher its absolute value, the faster and further the point will move. From the mathematical morphology point of view we make the radius of the structural circle depend on the absolute value of the

curvature. Now, can we assure, analytically speaking, that our evolution will stay smooth for all times?. On one hand we have that the equation (3) associated to θ in arc length parameter has turned into a PDE of parabolic elliptic type:

$$\theta_t = \theta_{ss} + (\int_0^s \theta_s^2 ds)\theta_s \ . \tag{6}$$

Hence by general theory on PDE's [7], we already know that our Curvature Distance Map (CDM) will be infinitely differentiable. Intuitively, the Laplacian that equation (6) contains introduces curvature into the characteristic lines, so that two characteristics do not intersect any more. Besides, the large amount of literature [9], [10], [11] on MCF, states that any initial curve evolves smoothly towards a convex shape, circular in the limit, before collapsing to a point. This is the key point to the definition of CDM.

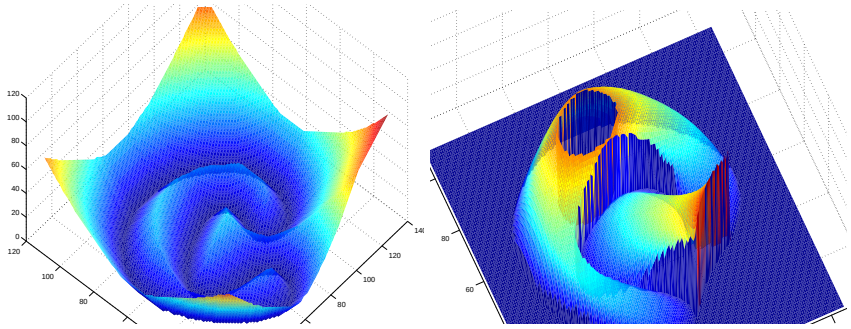

(a) (b)

Fig. 3. Detail of Euclidean distance map, showing a crest of positive slope (a) and detail of Elliptic Distance Map (b) .

Evolution by negative curvature $\gamma_t = \min((\kappa, 0))\overrightarrow{n}$ **Evolution by positive curvature** $\gamma_t = \max((\kappa, 0))\overrightarrow{n}$ (7)

We will define separately the outward and inward propagation in order to ensure maximal accuracy in the position of the snake. The analysis of Section 2.1 points out that convex shapes do not develop shocks during their propagation. An evolution of a non convex shape by negative curvature [17] stops as soon as the curve becomes convex. Therefore, for the outward propagation, we will evolve the initial shape under the flow given by (7) until it stabilizes. The tracking of the curve for each time produces the level sets of the outward CDM for the non convex regions. To complete the outward CDM, we use an outward Euclidean distance map to the stable state of the flow by negative curvature. For the inward propagation we use evolution under positive curvature (7) until the curve

becomes circular and then we use the Euclidean distance map to this circle to complete the inward propagation.

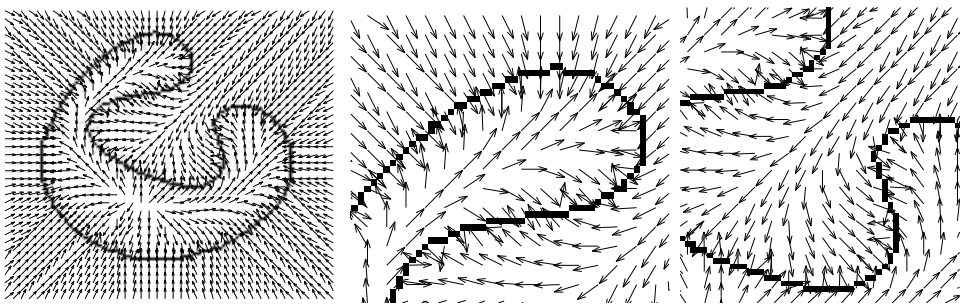

(a) (b) (c)

Fig. 4. Gradient of the Elliptic Distance Map (a) and close-ups from the interior (b) and exterior (c).

Since there are not any self intersections between the level curves of CDM, we obtain maps (fig. 3 (b)) without curves of null gradient or saddle points (fig. 4 (a)). The gradient of this map, CVF, drives the snake [5] to the zero level curve of CDM whatever its geometry. Details of CVF shown in figure 4 illustrate the absence of either saddle points or null gradients in both, the interior (fig. 4 (b)) and exterior (fig. 4 (c)) regions of a highly non-convex curve.

3 Applications to Shape Modelling

In this section we apply CVF to smooth shape representation. Given a closed curve in the plane, we approach it by means of a parametric B-spline snake that uses CVF as external force. In the case of discontinuous curves, CVF is computed over their closing obtained by dilation. We recall the reader that a parametric snake [14] is a curve $\gamma(u) = (x(u), y(u))$ that minimizes the energy functional:

$$E(\gamma) = \int_\gamma (E_{int} + E_{ext})du = \int_\gamma (\alpha||\gamma^{'}||^2 + \beta||\gamma^{''}||^2 + E_{ext})du \ ,$$

where the external energy depends on the image object to model and can be either a distance map or a function of the original image gradient. The parameters α and β determine the stiffness of the deformable model and are in the range $[0, 1]$. In any case the optimal curve is obtained by means of the Euler-Lagrange equations associated to E, which are equivalent to solving a linear system:

$$Ax = -\nabla E_{ext} \ .$$

The numeric iterative scheme is given by:

$$x_{t+1} = (A + \lambda I)^{-1} (\lambda x_t - \nabla E_{ext})$$

where I denotes the identity matrix, A the stiffness matrix [14] and λ is a viscosity parameter. An important remark is that stability of the finite difference scheme depends upon the viscosity parameter, which must be increased if α, β decrease. This viscosity parameter determines the speed of convergence, the higher it is, the slower the snake converges. We consider the snake has reached its final state when its total energy stabilizes.

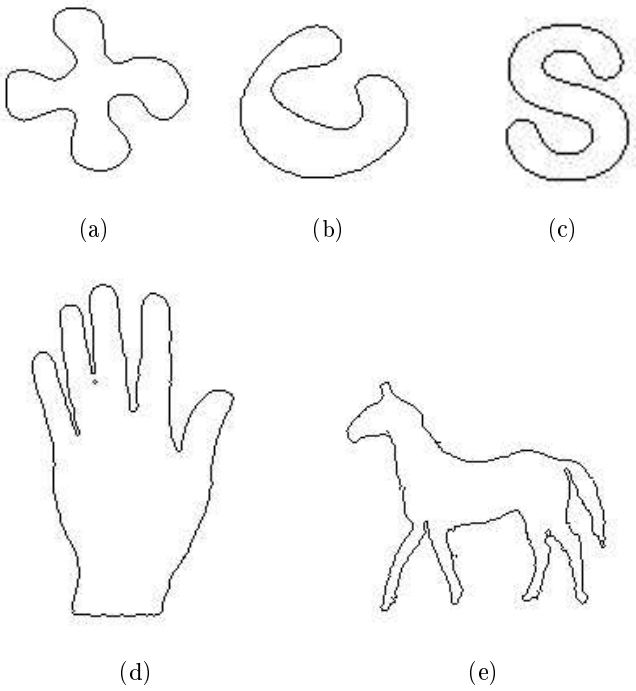

Fig. 5. Set of test shapes: clover (a), highly non-convex curve (b), character 'S' (c), hand (d) and horse (e).

3.1 Results

Experiments focus on the efficiency and accuracy of CVF when non-convex contours are modelled. Accuracy has been computed in terms of snake convergence, given by the snake maximum Euclidean distance to the original closed contours. Efficiency is given by the CPU-time the initial snake takes to reach its final state.

Since the stop criterion is in terms of the stabilization of the external energy, the asymptotic behavior of the functional E is also a measure of the method efficiency. An oscillating graph for E hinders stopping the deformable model with the former stop criterion and the final snake must be obtained after a fixed number of iterations.

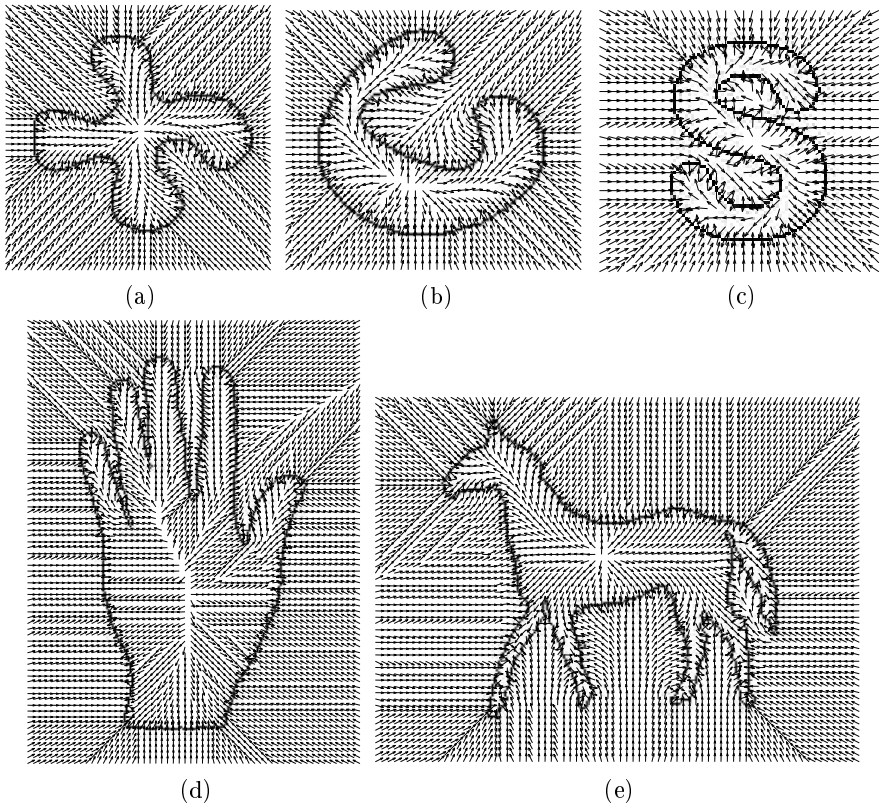

Fig. 6. CVF on clover (a), highly non-convex curve (b), character 'S' (c), hand (d) and horse (e).

We have tested the external potentials for different values of the snake parameters, α and β, in order to check if the energies could support large values and still guarantee convergence of the snake to the curve of interest. As noticed before, supporting large values for α, β is also a signal of efficiency, since the larger these parameters are, the faster the snake converges. The snake has been initialized inside and outside the object of interest. We have compared CVF to the results obtained using a GVF-regularized gradient of the Euclidean distance map (DM) and GVF applied to the edge map.

The shapes chosen are depicted in figure 5. The external force given by CVF is shown in figure 6. Convergence of snakes for the different external forces is shown in figure 9 and the final model obtained is depicted in figure 10.

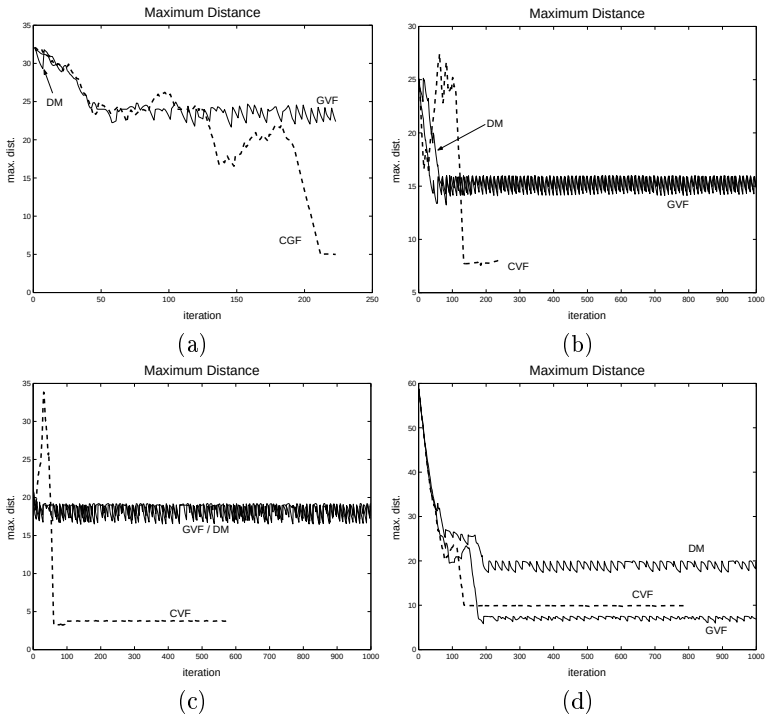

Fig. 7. Snake accuracy, interior convergence for highly non convex shape (a) and the clover (b) and the corresponding exterior convergence (c) and (d)

In terms of an accurate model of the shape, CVF is the only external energy that adapts the deformable model to all curves, whatever position (inside or outside the object of interest) of the initial snake. The other two external energies fail to obtain an accurate model when the initial snake lies inside the object of interest. Convergence to the character 'S' and horse in fig. 9 and the final shapes of fig. 10 illustrate this bad-pose of the snake inner convergence with GVF and DM. In the case of the character 'S', saddle points of both GVF and DM, make the snake oscillate at closed shapes which fail to reach the extremal boundary of the 'S'. Irregularities in the gradient of the horse external energy, produces open final snakes (fig. 10(b),(c)) approaching only a part of the animal's contour. Notice the accuracy and smoothness of the final model of the horse achieved with CVF (last row of fig. 10(a)). In the case of an outer initial snake, GVF succeeds in adapting to non convex shapes such that the angle θ does not turn

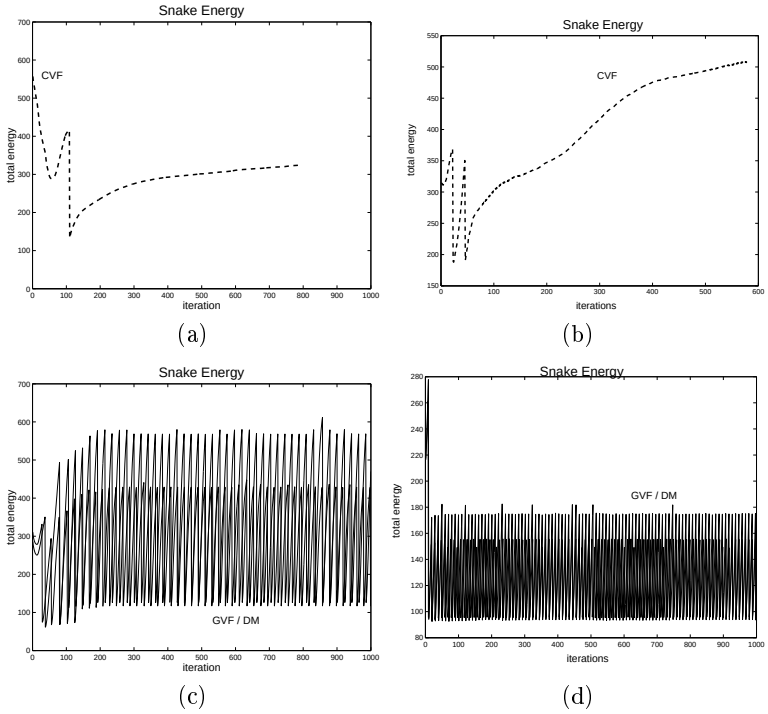

Fig. 8. Evolution of snake energy, CVF exterior convergence for highly non-convex shape (a), the clover (b) and the corresponding GVF/DM convergence (c) and (d)

more that π between two consecutive inflexion points (like the clover of fig. 10(b)). However the snake gets trapped at the saddle points that highly non convex shapes (second row of fig. 10(b)) produce in the vector field. The external force field obtained by a regularization of the gradient of DM using GVF is the worst performer. Even for small values of α and β, the external force is not strong enough to attract the snake to non-convex shapes, even in the case of shapes (like the clover of fig. 10(c)) with the angle θ turning less than π between two consecutive inflexion points. Figure 7 summarizes these results in the form of maximum Euclidean distance to the contour of interest versus number of iterations. Notice significant differences of the maximum distance between CVF and DM/GVF in the case of convergence to highly non-convex shapes (fig. 7 (a),(c)).

Concerning efficiency, CVF is, again the best performer, since attains accurate models in optimal time, meanwhile GVF is the worst of the methods. Times for DM have not been taken into account since the method does not produce good enough segmentations as to be taken into account. The main reason for this difference in times lies on the fact that, due to the smoothness of the map, deformable models guided by CVF do not need, in general to be re sampled

during evolution. On the other side, since GVF does not take into account the geometry of shapes, the snake sampling must be refined at points where two opposite directions compete (that is when entering into concave regions) in order to guarantee convergence to a closed contour. This increases the computational time of GVF up to four times CVF time in the case of the hand or the horse. Also in terms of the stiffness parameters, α and β, CVF is the most efficient. Our tests done for different values of the stiffness parameters show that CVF supports, in general, values in the whole range of $[0, 1]$. Only in extreme cases like inner convergence to the horse and outer convergence to the hand, α and β must be smaller than 0.3 if we want a reliable final model.

Another issue worth to be considered is the asymptotic behavior of the snake convergence. Figure 8 shows the evolution of the snake energy in time for convergence to the clover and the highly non-convex shape of fig. 9, in the case of a CVF guided snake (fig. 8(a),(b)) and a DM/GVF one (fig. 8(c),(d)). Notice that deformations under CVF present a smoother asymptotic behavior, compared to the highly oscillating graphics of DM and GVF. This oscillating behavior strengths when the snake gets trapped at saddle points. A smooth energy implies a strong advantage since a stop criterion in terms of the snake total energy is a robust way of determining the final state for CVF guided snakes.

4 Conclusions and Future Work

Shape modelling and reconstruction is an issue frequently addressed in different fields of computer vision and graphics. Snakes or deformable models are a common way of obtaining smooth shape models. The external force is crucial in order to ensure the snake convergence. In the present paper we have introduced a new distance map to closed contours. Based on the grounds that a distance map represents the evolution of an initial curve in time under a geometric PDE, we propose using the mean curvature flow to avoid shock formation. The gradient of this map is a smooth external force that guides in a natural manner the snake to the shape of interest. The fact that the force field takes into account the geometry of the final curve, makes convergence robust whatever the concavity of this curve is. The only requirement is that the initial snake must be either inside or outside the shape of interest. Experiments show the higher accuracy and efficiency of our model of shapes compared to the most commonly used external force fields in the framework of parametric snakes. Comparing to geodesic active contours, our CVF converges faster to a comparable segmenting snake.

We are aware that requiring closed contours is a main limitation of CVF. However we argue that ensuring convergence and a smooth potential should be essential requirements for any external energy. In order to apply CVC to object segmentation, special treatment must be made to noisy images well as to uncompleted contours. In [6] we present a more general framework for segmentation purposes where we embed CVF to segment real images with concave objects.

References

1. V. Caselles, F. Catte, T. Coll, F. Dibos, *A geometric model for active contours.* Numerische Mathematik, 66, pg.1-31, 1993.
2. V. Caselles, R.Kimmel, G. Sapiro *Geodesic Active Contours.* Int. J. Comp. Vision.
3. L.D. Cohen, R. Kimmel, *Global minimum for active contour models: A minimal path approach.* Int. Journal Comp. Vision, 24 (1), pp. 57-78, Aug. 1997.
4. D. Gil, P. Radeva. *Regularized curvature flow.* CVC Tech. Report n^o 63, 2002.
5. D. Gil, P. Radeva. *Curvature based Distance Maps.* CVC Tech. Report n^o 70, 2003.
6. D. Gil, P. Radeva. *Anisotropic Contour Completion*, ICIP'03 (submmited).
7. L.C. Evans. *Partial Differential equations.* Berkeley Math. Lect. Notes, vol. 3B.
8. D.R. Forsey, R.H. Bartels. *Surface Fitting with Hierarchical Splines*, Computer Graphics, April 1995.
9. M.A. Grayson. *The heat equation shrinks embedded plane curves to round points.* J. Differential Geometry, Vol. 26, pp. 285-314, 1986.
10. M. Gage, R.S. Hamilton. *The heat equation shrinking convex plane curves.* J. Differential Geometry, Vol. 23, pp. 69-96, 1986.
11. M. Gage. *Curve shortening makes convex curves circular.* Invent. Math, vol 76, pp. 357-364, 1984.
12. F.Guichard, J.M.Morel *Mathematical Models in Image Processing.* Advanced Courses on Mathematical Aspects on Image Processing.
13. H. Hoppe, T. DeRose, T. Duchamp, M. Halstead, H. Jin, J. McDonald, J. Scheweitzer, and W. Stuetzle, *Piecewise smooth surface reconstruction*, Proc. ACM SIGGRAPH, pp. 295-302, July 1994.
14. M.Kass, A.Witkin and D.Terzopoulos, "Snakes: Active Contour Models", *Int. Journal of Computer Vision*, vol. 1, pp. 321-331, 1987.
15. Ch. Knoll, M. Alcañiz, V. Grau, C. Montserrat, M.C. Juan, *Outlining of the prostate using snakes with shapes restrictions based on the wavelet transform.* Pattern Recognition, 32, pp. 1767-1781, 1999.
16. W. Rudin. *Complex and Real Analysis.* McGraw-Hill, Inc.
17. R.Malladi, J.A. Sethian. *Image Processing: Flows under min-max curvature and mean curvature.* Graph. Models and Image Process., vol. 58 (2), Mar. 1996.
18. G. Sapiro, B.B. Kimia, R. Kimmel, D. Shaked, A. Bruckstein. *Implementing continuous-scale morphology.* Pattern Recognition, vol. 26(9), 1992.
19. K. Siddiqi, A. Tannenbaum, S.W. Zucker. *A Hanmiltonian Aaproach to the Eikonal Equation*, EMMCVPR'99, Lecture Notes in comp. Science, 1654.
20. Ch.Sun, S. Pallotino, *Circular shortest path on regular grids*, Asian Conference on Computer Vision, pp. 852-857, Melbourne, Australia, Jan. 2002.
21. Z.S.G. Tari, J. Shah, H. Pien. *Extraction of shape skeletons from grayscale images.* Comp. Vision and Image Understanding, vol. 66, pp. 133-146, May 1997.
22. C.Xu and J.L. Prince *Snakes, shapes and gradient vector flow.* IEEE Trans. on Image Proc., vol. 7(3), pp. 359-369, March 1998.
23. N.Paragios, O.Mellina-Gottardo, V.Ramesh, *Gradient Vector Flow Fast Geodesic Active Contours.* Comp. Vision, ICCV 2001.
24. C.Xu and J.L. Prince *Generalized gradient vector flow external forces for active contours.* Signal Processing, An International Journal, vol. 71(2), pp. 132-139, 1998.
25. D. Zhang, M. Herbert, *Harmonic shape images: a representation for 3-d free-form surfaces based on energy minimization*, EMMCVPR'99, Lect. Notes in Comp. Science, 1654.

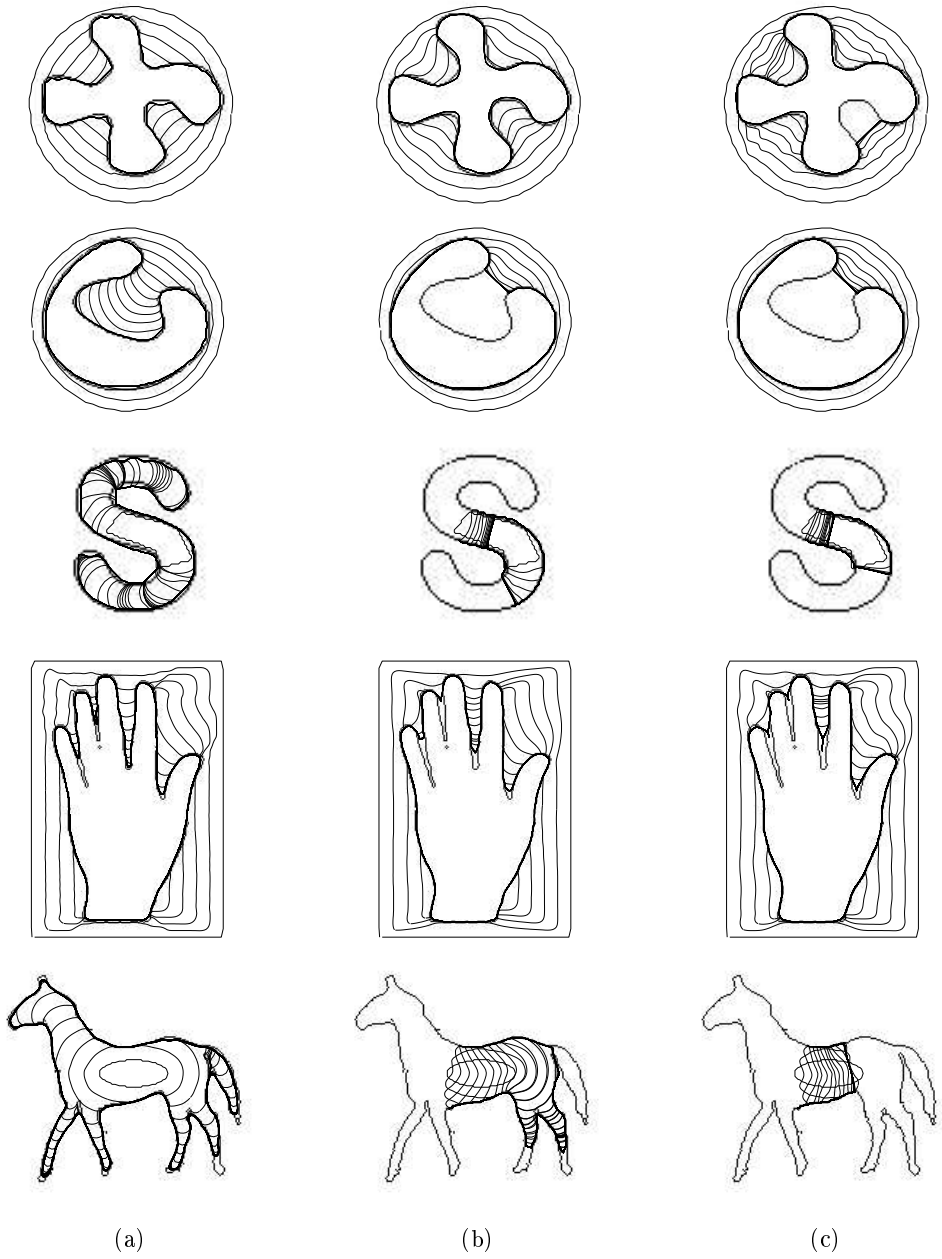

Fig. 9. Snake convergence, CVF (a), GVF (b) and regularized DM (c).

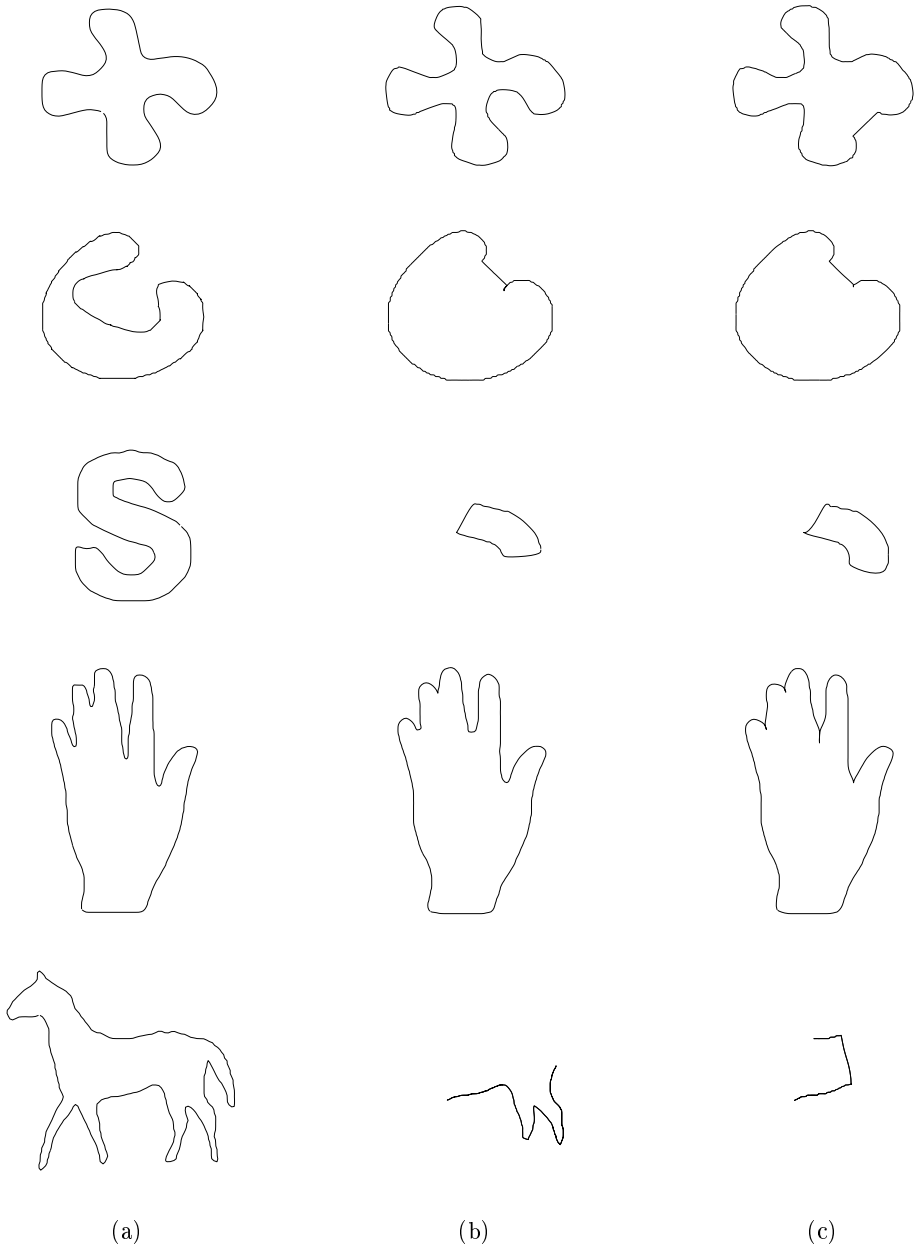

Fig. 10. Models of shapes obtained with CVF (a), GVF (b) and regularized DM (c).